Available online at www.sciencedirect.com
ScienceDirect
Catalysis Today 126 (2007) 81–89
CATALYSIS TODAY
www.elsevier.com/locate/cattod

# Combined *in situ* FT-IR and TRM analysis of the $NO_x$ storage properties of Pt-Ba/$Al_2O_3$ LNT catalysts

F. Frola[a], F. Prinetto[a,*], G. Ghiotti[a], L. Castoldi[b], I. Nova[b], L. Lietti[b], P. Forzatti[b]

[a] *Dipartimento di Chimica IFM, Università di Torino, and INSTM Consortium, UdR Torino, Via P. Giuria 7, 10125 Torino, Italy*
[b] *Dipartimento di Chimica, Materiali e Ingegneria Chimica "Giulio Natta", Centro NEMAS-Nano Engineered Materials and Surfaces Politecnico di Milano, Piazza Leonardo da Vinci 32, 20133 Milano, Italy*

## Abstract

The storage of $NO_2$ and NO/$O_2$ in the presence and in the absence of $CO_2$ was investigated at 350 °C on Pt-Ba/$Al_2O_3$ LNT catalysts and on the reference Ba/$Al_2O_3$ system, by coupling *in situ* FT-IR spectroscopy and transient response method (TRM). Experiments were performed by admitting $NO_2$/$CO_2$ or NO/$O_2$/$CO_2$ mixture ($CO_2$/$NO_x$ ratios in the range 1–7) or, in alternative, by admitting $NO_2$ or NO/$O_2$ on catalysts previously saturated by flowing $CO_2$.

In the case of $NO_2$/$CO_2$ adsorption, it was found that $NO_2$ was efficiently stored as nitrate species according to a disproportion reaction, which occurs with evolution of NO, as in the absence of $CO_2$.

In the case of NO/$O_2$/$CO_2$ adsorption it was confirmed that two pathways operated simultaneously as in the absence of $CO_2$: the "nitrite route", involving the initial formation of surface nitrite and their subsequent evolution to nitrates, and the "nitrate route", involving NO oxidation to $NO_2$ over Pt and its subsequent adsorption on Ba in the form of nitrates. The presence of $CO_2$ inhibits to some extent the "nitrite route", whereas the "nitrate route" proceeds as in the absence of $CO_2$.

*Keywords:* $NO_x$ storage; Lean $NO_x$ Trap; Pt-Ba/$Al_2O_3$; Transient response method; FT-IR spectroscopy; $CO_2$

## 1. Introduction

The need of developing new catalytic systems efficient in the reduction of $NO_x$ under lean conditions is a current challenge. An interesting solution is represented by the so-called "$NO_x$ storage-reduction catalysts" or "Lean $NO_x$ Traps" (LNT), constituted by a $NO_x$-storage component (typically an alkaline or earth-alkaline metal oxide) and by a noble metal (Pt) which operates the $NO_x$ reduction [1–4]. Several papers have been recently published on these catalytic systems, and both the storage and the reduction phases have been investigated [5–8], although some mechanistic aspects still remain controversial. In this frame, an extensive investigation was carried in our labs, with the aim of elucidating the $NO_x$-storage mechanism on Pt-Ba/$Al_2O_3$ catalysts. *In situ* FT-IR spectroscopy and the transient response method (TRM) proved to be very useful techniques to gain complementary information on surface species and gas phase composition, which allowed the proposal of a novel pathway for $NO_x$ storage upon admission of NO/$O_2$ mixtures [9–11]. It was indeed shown that the NO/$O_2$ storage proceeds through two parallel routes: (i) the "nitrite route", which implies NO storage on Ba neighbouring Pt sites in the form of nitrite ad-species that are then progressively oxidized to nitrates; (ii) the "nitrate route", implying NO oxidation to $NO_2$ on Pt sites, followed by $NO_2$ disproportion on Ba sites with formation of nitrates and NO release in the gas phase.

In order to better approach the real working conditions of the LNT catalysts in the engines, and to understand if the presence of $CO_2$ could alter the proposed storage pathways, this paper addresses the effects of the presence of $CO_2$ on the efficiency of the $NO_x$ storage and on the $NO_x$ storage mechanisms, again by coupling *in situ* FT-IR spectroscopy and TRM technique over model Pt-Ba/$Al_2O_3$ catalysts and, for comparative purposes, over the binary Ba/$Al_2O_3$ reference sample.

---

[*] Corresponding author. Tel.: +39 0116707539; fax: +39 0116707855.
*E-mail address:* federica.prinetto@unito.it (F. Prinetto).

0920-5861/$ – see front matter © 2006 Elsevier B.V. All rights reserved.
doi:10.1016/j.cattod.2006.10.010

## 2. Experimental

### 2.1. Materials and techniques

Homemade Pt-Ba/$Al_2O_3$ catalysts (1–16/100) were prepared by impregnation of γ-alumina in two sequential steps as follows. A powder γ-$Al_2O_3$ carrier (Versal 250 from La Roche Chemicals, surface area of 200 $m^2$/g and pore volume of 1.2 $cm^3$/g) was at first impregnated with a solution of $Pt(NH_3)_2(NO_2)_2$ (Strem Chemicals, 5% Pt in ammonium hydroxide) with an appropriate concentration so as to yield 1 wt% Pt metal loading. After drying in air for 12 h at 80 °C and calcination at 500 °C for 5 h, batches of this sample were impregnated with a $Ba(CH_3COO)_2$ solution (Strem Chemicals, 98.5%) so as to yield Ba loading of 16 wt%. The impregnated sample were initially dried for 12 h at 80 °C and then calcined at 500 °C for 5 h.

For comparative purposes, the reference binary systems, Pt/$Al_2O_3$ (1/100) and Ba/$Al_2O_3$ (16/100) were also prepared using the same precursors and procedures.

Surface area and pore size distribution were determined by $N_2$ adsorption–desorption at 77 K with the BET method using a Micromeritics TriStar 3000 Instrument.

The Pt dispersion was estimated from hydrogen chemisorption at 0 °C after reduction in $H_2$ at 300 °C using a TPD/R/O 1100 ThermoElectron Corporation Instrument.

XRD spectra were collected on powder samples calcined at 500 °C with a Brüker D8 Advanced Instrument equipped with graphite monochromator on the diffracted beam.

### 2.2. Study of the $NO_x$ storage

The adsorption of $NO_x$ on Ba/$Al_2O_3$ and Pt-Ba/$Al_2O_3$ under transient conditions has been investigated by *in situ* FT-IR spectroscopy and by the transient response method. In both cases, $NO_x$ storage data reported were obtained on samples that were fully conditioned by performing few previous storage–regeneration cycles, consisting of heating in $NO_2$ at 350 °C and desorption at 600 °C [12].

Absorption/transmission IR spectra were run on a Perkin-Elmer FT-IR System 2000 spectrophotometer equipped with a Hg–Cd–Te cryo-detector, working in the range of wavenumbers 7200–580 $cm^{-1}$ at a resolution of 1 $cm^{-1}$ (number of scans ~10). For IR analysis powder samples were compressed in self-supporting discs (10 mg $cm^{-2}$) and placed in a commercial heatable stainless steel cell (Aabspec) allowing thermal treatments *in situ* under vacuum or controlled atmosphere and the simultaneous registration of spectra at temperatures up to 600 °C. Pellets were fully conditioned as previously described, then heated in dry $O_2$ at 600 °C, cooled down to 350 °C and evacuated at the same temperature. $NO_x$ storage experiments were performed by admitting $NO_2$ or freshly prepared NO/$O_2$ 1:4 mixtures (NO freshly distilled before use) at 350 °C in the presence of $CO_2$ ($CO_2$/$NO_x$ ratios in the range 1–7). All gases were from Praxair. IR spectra were recorded at the same temperature (350 °C) at increasing exposure times to the various gaseous mixtures.

For comparative purposes, the adsorption of $CO_2$ at 350 °C at increasing pressure and exposure time in the absence of $NO_x$ was also studied.

In another series of IR experiments, $NO_2$ or NO/$O_2$ adsorption was carried out at 350 °C on samples previously saturated by flowing $CO_2$ and then evacuated at the same temperature. In all experiments, the catalyst regeneration (*i.e.* the removal of the stored $NO_x$) was accomplished by treatment with $H_2$ at 350 °C or, in alternative, by desorption at increasing temperature.

For TRM experiments a flow micro-reactor system made of a quartz tube (7 mm i.d.) inserted into an electric furnace driven by a PID temperature controller/programmer was used. The temperature of the catalyst was measured and controlled by a K-type thermocouple (o.d. = 0.5 mm) directly immersed in the catalyst bed. The flow rate of the feed gases was measured and controlled by mass-flow controllers (Brooks 5850 TR), and the gases were mixed in a single stream before entering the reactor. Two four-port valves were used to perform the abrupt switches in the inlet gas phase composition. The reactor outlet was directly connected to a mass spectrometer (Balzers QMS 200); care was taken to minimize all possible dead volumes in the lines before and after the reactor and in eliminating pressure and flow changes upon switching of the feed gases. The following mass-to-charge (*m*/*e*) ratios were used to monitor the concentration of products and reactants: 18 ($H_2O$), 28 ($N_2$ or CO), 30 (NO), 32 ($O_2$), 44 ($N_2O$ or $CO_2$), and 46 ($NO_2$). The mass-spectrometer data were quantitatively analyzed using the fragmentation patterns and the response factors determined experimentally from calibration gases. A gas chromatograph (HP 6890) equipped with a Poraplot Q and a 5 Å molecular sieve capillary column was also used for the analysis of $CO_2$, $N_2O$, and $H_2O$, and of $O_2$, $N_2$, and CO, respectively.

In a typical experiment, 60 mg of catalyst sample were loaded in the reactor and heated at 350 °C in He or He + 3% $O_2$ (100 N $cm^3$/min at Standard Temperature Pressure, STP). After stabilisation of the mass-spectrometer signals, a rectangular step feed of NO (1000 ppm in He + $O_2$) or $NO_2$ (1000 ppm in He) was admitted at constant temperature. The $NO_x$ storage was allowed to proceed up to catalyst saturation; then the inlet $NO_x$ concentration was stepwise decreased to zero. The subsequent catalyst regeneration was accomplished by TPD: the catalyst was cooled to room temperature in He (flow rate of 100 $cm^3$/min) and then linearly heated to 600 °C at 10 °C/min, followed by a hold at 600 °C.

Analogous TRM experiments were carried out in the presence of $CO_2$ (0.3%, v/v) at 350 °C. Finally, for comparative purposes, $NO_2$ or NO/$O_2$ adsorption at 350 °C on samples previously saturated by flowing $CO_2$ (0.3%, v/v) was also studied.

## 3. Results and discussion

### 3.1. Catalyst characterization

The main chemical, textural and morphological features of the Pt-Ba/$Al_2O_3$ catalyst and of the binary Pt/$Al_2O_3$ and Ba/$Al_2O_3$ reference materials are reported in Table 1. Further

Table 1
Chemical composition, textural and morphological features of the fresh materials

| Sample | Pt content (%, w/w) | Ba content (%, w/w) | Surface area ($m^2$/g) | Pore volume ($cm^3$/g) | Pt dispersion (%) | Crystalline phases |
|---|---|---|---|---|---|---|
| $Pt/Al_2O_3$ | 0.99 | 0 | 186 | 1.02 | 82 | $\gamma$-$Al_2O_3$[a] |
| $Pt$-$Ba/Al_2O_3$ | 0.83 | 16.5 | 137 | 0.81 | 71 | $\gamma$-$Al_2O_3$[a], $BaCO_3$[b] |
| $Ba/Al_2O_3$ | 0 | 16.7 | 133 | 0.82 | – | $\gamma$-$Al_2O_3$[a], $BaCO_3$[b] |

[a] $\gamma$-$Al_2O_3$, JCPDS no. 10-425.

[b] $BaCO_3$ orthorombic, JCPDS no. 5-378, and monoclinic, JCPDS no. 78-2057.

details on the characterization of the samples can be found in previous papers [9,12,13]. Quantitative analysis of the X-ray diffractograms indicated that in fresh $Ba/Al_2O_3$ and $Pt$-$Ba/Al_2O_3$ samples, nearly 30% of Ba is present as crystalline $BaCO_3$, the remaining fraction being likely present as highly dispersed Ba carbonate or Ba oxide.

The presence of bulky $BaCO_3$ on the fresh $Ba/Al_2O_3$ and $Pt$-$Ba/Al_2O_3$ samples is also clearly revealed by IR bands at 1440 $cm^{-1}$ with shoulders at 1550, 1400 and 1370 $cm^{-1}$ (Fig. 1A curve 1 for $Pt$-$Ba/Al_2O_3$ sample) [14].

After few cycles of $NO_x$ adsorption at 350 °C and regeneration by heating at 600 °C, both in IR spectra (Fig. 1A) and in XRD patterns (Fig. 1B) the features due to crystalline $BaCO_3$ disappeared, while no new crystalline Ba phases were detected. This accounts for an almost complete evolution of $BaCO_3$ to $Ba(NO_3)_2$, which was then decomposed into a dispersed nanosized BaO phase [18–20]. Notably, this evolution occurs at temperatures markedly lower than those required for the thermal decomposition of bulk $BaCO_3$ [12,15]. In agreement, TRM data collected during the initial $NO_x$ storage–regeneration cycles onto fresh catalysts showed a significant evolution of $CO_2$ [21]. After three cycles $CO_2$ is no more detected at the reactor outlet, suggesting that the transformation of barium carbonate into barium oxide is almost complete. Samples were thus hereafter conditioned by performing few $NO_x$ adsorption–regeneration cycles before studying $NO_x$ storage.

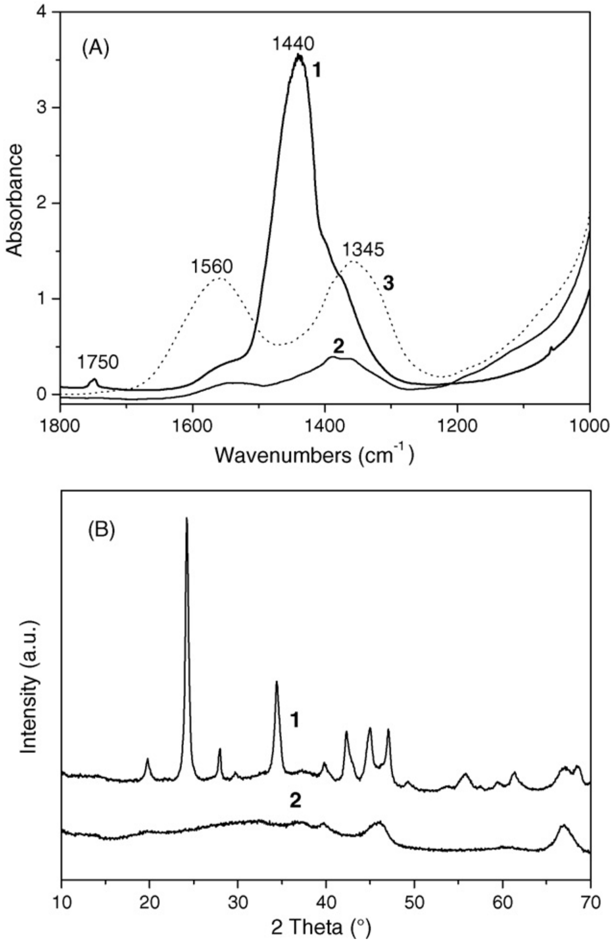

Fig. 1. (Section A) Absorbance FT-IR spectra recorded at 350 °C of fresh $Pt$-$Ba/Al_2O_3$ catalyst (curve 1); thereafter submitted to conditioning treatment (curve 2); and after the subsequent admission of $CO_2$ at saturation (20 mbar, curve 3). (Section B) XRD patterns of fresh $Pt$-$Ba/Al_2O_3$ catalyst (curve 1); thereafter submitted to conditioning treatment (curve 2).

## 3.2. Study of $NO_x$ storage in the presence of $CO_2$

### 3.2.1. Adsorption of $CO_2$

In order to point out the effect of $CO_2$ on the $NO_x$ storage, we have firstly studied the adsorption of $CO_2$ in the absence of $NO_x$ on conditioned $Ba/Al_2O_3$ and $Pt$-$Ba/Al_2O_3$ catalysts, at increasing pressure and contact time, at the same temperature (350 °C) used in $NO_x$ adsorption experiments.

A relevant point is that surface species formed upon $CO_2$ adsorption exhibit spectral features completely different from those of crystalline $BaCO_3$ present on the fresh sample (compare curves 1 and 3 in Fig. 1A).

To better appreciate the spectral features upon $CO_2$ adsorption, in Fig. 2 we have reported the difference spectra, *i.e.* after subtraction of the spectrum before $CO_2$ admission. Absorptions at 1560, 1345 and 1060–1050 $cm^{-1}$ were observed to form upon $CO_2$ admission, which are characteristic of surface bidentate carbonate species adsorbed on the Ba phase ($\nu_{C=O}$, $\nu_{OCO}$ asym and $\nu_{OCO}$ sym, respectively) [16]. Notably, no surface species typical of $CO_2$ adsorption on the alumina support were detected, such as organic-like carbonates (observed at 1860–1780, 1200–1180 $cm^{-1}$ in the case of the $Pt/Al_2O_3$ reference sample, spectrum not reported) and hydrogen carbonates (observed at 1680–1640, 1480, 1240 $cm^{-1}$ on $Pt/Al_2O_3$) [17]. This accounts for an extensive spreading of the barium oxide phase over the support, as previously suggested [12].

Carbonate species formed on $Ba/Al_2O_3$ and $Pt$-$Ba/Al_2O_3$ were similar, except for the presence of an additional component at 1445 $cm^{-1}$ in the case of the binary system, due to small amounts of monodentate species.

Finally, carbonate species formed upon $CO_2$ adsorption exhibited a moderate thermal stability, being almost completely

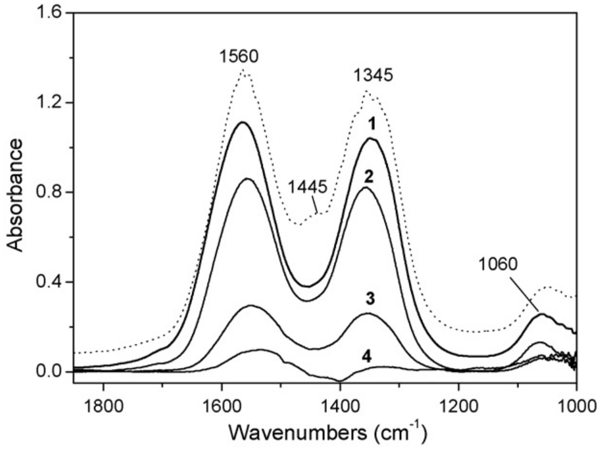

Fig. 2. FT-IR spectra of Pt-Ba/$Al_2O_3$ catalyst upon admission of 20 mbar of $CO_2$ at 350 °C (curve 1) and subsequent evacuation at 350, 450, 550 °C (curves 2, 3 and 4, respectively). For comparison, admission of 20 mbar of $CO_2$ at 350 °C on Ba/$Al_2O_3$ (dotted line). Spectra have been reported after subtraction of the spectrum before $CO_2$ admission.

removed by evacuation at 550 °C, as seen from spectra in Fig. 2 and from Fig. 3, where the integrated intensities of the overall absorption in the range 1700–1100 $cm^{-1}$ have been reported as a function of the evacuation temperature.

All these findings mean that, once decomposed by the conditioning treatment, the crystalline $BaCO_3$ phase present on the fresh samples is not readily restored by $CO_2$ interaction.

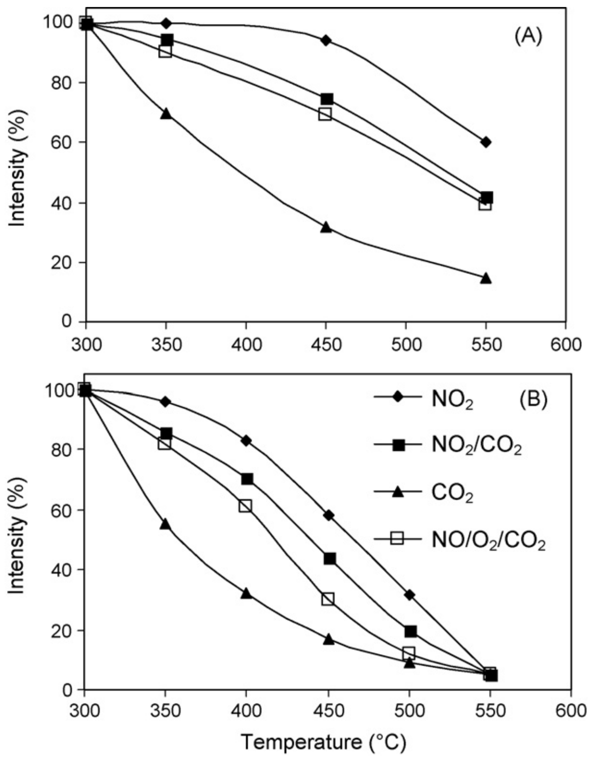

Fig. 3. Thermal stability of species formed upon adsorption of $NO_2$ (◆), $CO_2$ (▲), $NO_2/CO_2$ 1:5 mixtures (■), NO/$O_2$/$CO_2$ 1:4:5 mixtures (□) on Ba/$Al_2O_3$ and Pt-Ba/$Al_2O_3$ samples (Sections A and B, respectively), evaluated by the integrated intensities of the IR absorptions in the 1700–1100 $cm^{-1}$ range *vs.* the evacuation temperature. The integrated intensity of the bands present at 300 °C has been put equal to 100%.

### 3.2.2. Adsorption of $NO_2$ in the presence of $CO_2$

In Fig. 4A the IR difference spectra obtained after admission of a $NO_2/CO_2$ 1:5 mixture at 350 °C on Pt-Ba/$Al_2O_3$ catalyst are compared with those obtained upon admission of the single gases, $NO_2$ and $CO_2$, in the same conditions of temperature, partial pressure and exposure time (2 min). It can be easily noted that the surface situation reached upon admission of the $NO_2/CO_2$ mixture (Fig. 4A, curve 1) closely resembles that obtained upon admission of $NO_2$ in the absence of $CO_2$ (Fig. 4A, curve 2). In particular, in both cases mainly nitrates are present at the catalyst surface, primarily of the ionic type (1410, 1320 and 1020 $cm^{-1}$) and in minor amounts bridging species (1550 $cm^{-1}$) [9,12]. In both cases nitrite formation is not observed.

Upon admission of the $NO_2/CO_2$ mixture, only small amounts of carbonates are formed, in spite of the large amounts of $CO_2$ in the gas phase, as indicated by the weak intensity of the mode at 1060 $cm^{-1}$. Note incidentally that the analysis of IR modes at wavenumbers lower than 1100 $cm^{-1}$ can be useful to solve the problem of the heavy superposition of vibrational

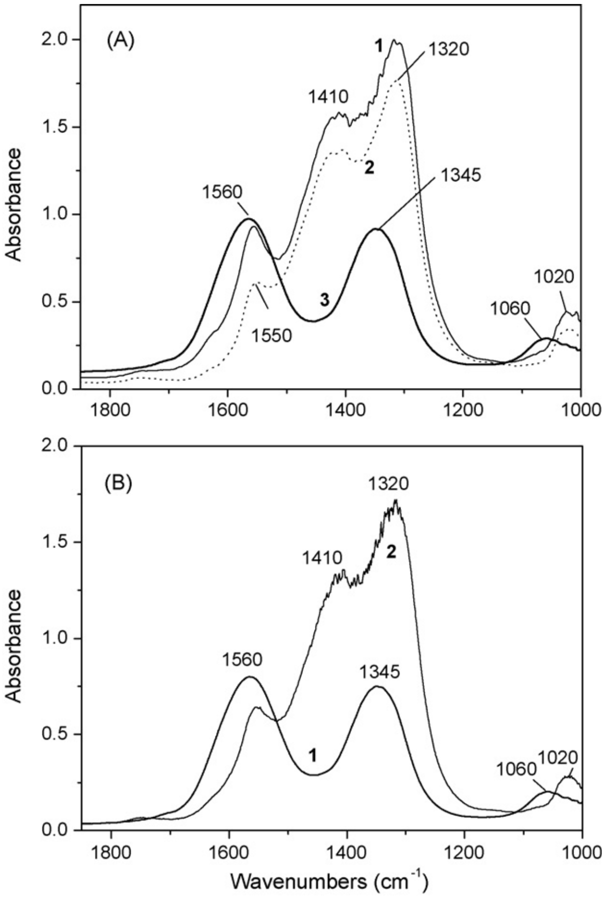

Fig. 4. FT-IR spectra of Pt-Ba/$Al_2O_3$ catalyst. (Section A) Admission of 24 mbar of $NO_2/CO_2$ 1:5 mixture at 350 °C (curve 1) after 2 min of contact; for comparison, admission of 4 mbar of $NO_2$ (curve 2) and of 20 mbar of $CO_2$ (curve 3) at the same temperature and contact time. (Section B) Admission of 20 mbar of $CO_2$ at 350 °C and subsequent evacuation at 350 °C (curve 1); subsequent admission of 4 mbar $NO_2$ at 350 °C (curve 2) after 2 min of contact. Spectra have been reported after subtraction of the spectrum before gas admission.

modes of $CO_3^{2-}$ and $NO_3^-$ in the 1700–1200 $cm^{-1}$ region. Indeed, carbonates exhibit the $\nu_{OCO}$ sym mode at 1060–1050 $cm^{-1}$, while the analogous $\nu_{ONO}$ sym mode of nitrates is shifted at 1030–1020 $cm^{-1}$.

Similar results were obtained for the binary $Ba/Al_2O_3$ sample (spectra not reported).

A good tool to evaluate the relative amounts of surface carbonate and nitrate species formed upon admission of the $NO_2/CO_2$ mixture is the analysis of the thermal stability of the surface species, especially at temperatures around 450 °C. Indeed it is noted from Fig. 3 that after admission of the $NO_2/CO_2$ mixture and subsequent evacuation at 450 °C, the overall intensity of the envelope of bands at 1700–1100 $cm^{-1}$ decreased of around 25% and 45% for the binary and the ternary systems, respectively. These intensity decreases are quite similar to those obtained in the case of admission of pure $NO_2$ (around 10 and 40% for the binary and the ternary systems, respectively). As seen, nitrates showed a lower stability in the case of the ternary system, which has been previously ascribed to the catalytic effect of Pt in nitrate decomposition [12].

At variance, surface carbonates formed upon admission of pure $CO_2$ showed a moderate stability, 70–80% being already desorbed upon evacuation at 450 °C. This further evidences that mainly nitrates are formed at the catalyst surface when $NO_2$ is admitted in the presence of $CO_2$.

In another series of experiments, $NO_2$ was admitted on the catalyst surface, which had been previously saturated by $CO_2$ at 350 °C and thereafter evacuated at the same temperature (Fig. 4B for $Pt\text{-}Ba/Al_2O_3$ sample). It appears that pre-existing surface carbonates were almost completely displaced by $NO_2$, as indicated by the marked decrease of the bands at 1560 and 1060 $cm^{-1}$, while nitrate formation proceeded. After few minutes of contact the situation was thus similar to that obtained upon $NO_2$ adsorption on the clean surface, *i.e.* presence of nitrates, primarily of the ionic type and in minor amounts of the bridging type, no nitrite formation.

Similar results were obtained for the binary $Ba/Al_2O_3$ sample (spectra not reported).

In agreement with IR data, TRM runs performed on the ternary $Pt\text{-}Ba/Al_2O_3$ catalyst (Fig. 5) showed that the adsorption capacity upon $NO_2$ adsorption over the clean and over the $CO_2$ pre-saturated surfaces are similar and only slightly decreased in the case of the $NO_2/CO_2$ mixture (see also Table 2).

From Fig. 5, it clearly appears that in all cases $NO_2$ adsorption is accompanied by NO evolution. As discussed elsewhere [9,10] NO formation is related to the occurrence of the following $NO_2$ dismutation reaction:

$$BaO + 3NO_2 \rightarrow Ba(NO_3)_2 + NO \tag{1}$$

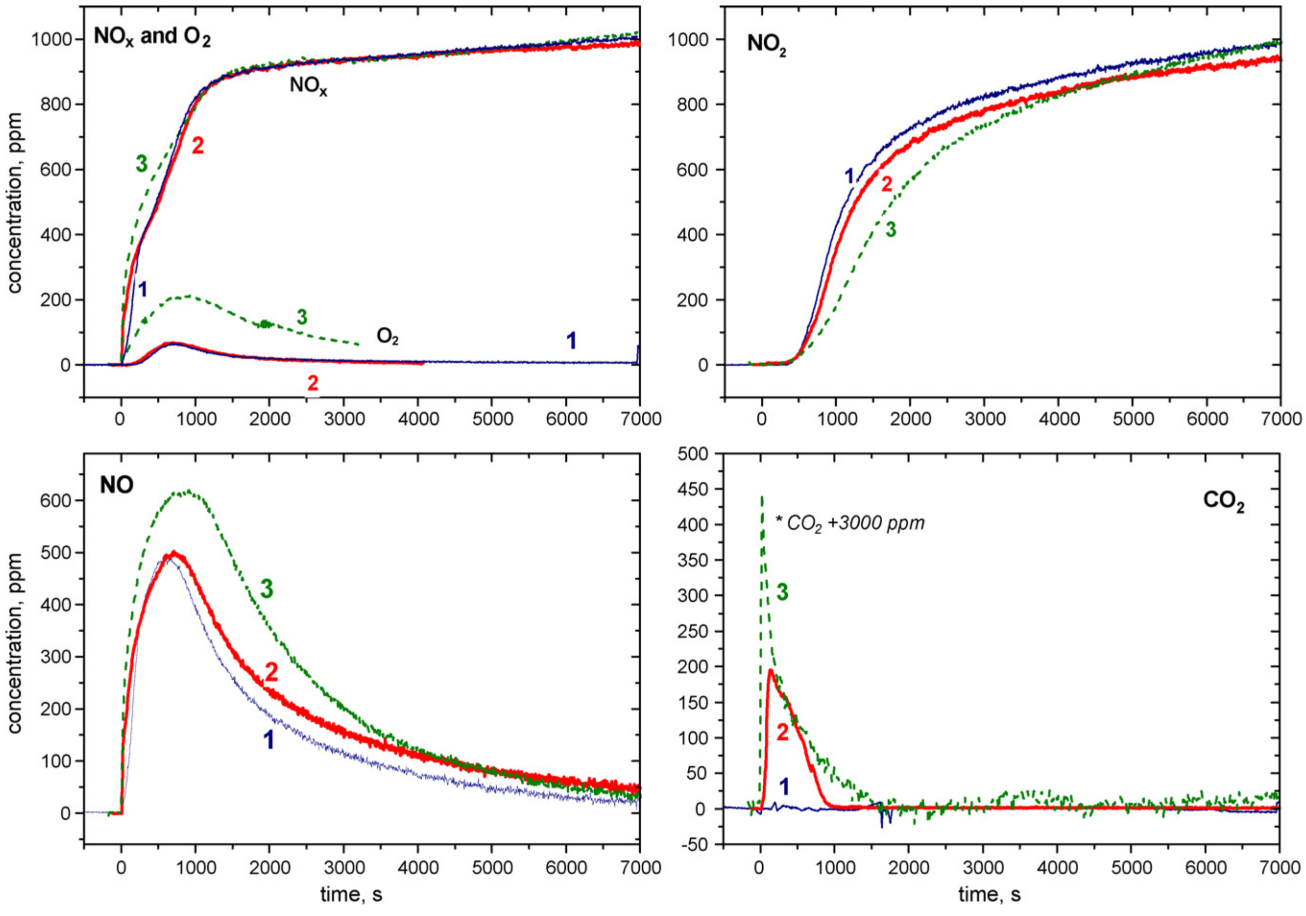

Fig. 5. $NO_x$, $NO_2$, NO, $CO_2$ outlet concentration *vs.* time on $Pt\text{-}Ba/Al_2O_3$ catalyst determined by TRM experiments at 350 °C upon admission of $NO_2$ (curve 1), of $NO_2$ on $CO_2$ pre-covered sample (curve 2) and of $NO_2/CO_2$ mixture (curve 3).

Table 2
Amounts of $NO_x$ adsorbed and $CO_2$ released during TRM experiments on $Ba/Al_2O_3$ and $Pt\text{-}Ba/Al_2O_3$ catalysts

| Experiment | $NO_2$ storage | | | | $NO/O_2$ storage | | | |
|---|---|---|---|---|---|---|---|---|
| | $NO_x$ adsorbed (mol/g cat) up to surface saturation | | $CO_2$ released (mol/g cat) | | $NO_x$ adsorbed (mol/g cat) up to surface saturation | | $CO_2$ released (mol/g cat) | |
| | $Pt\text{-}Ba/Al_2O_3$ | $Ba/Al_2O_3$ | $Pt\text{-}Ba/Al_2O_3$ | $Ba/Al_2O_3$ | $Pt\text{-}Ba/Al_2O_3$ | $Ba/Al_2O_3$ | $Pt\text{-}Ba/Al_2O_3$ | $Ba/Al_2O_3$ |
| $NO_x$ | 1.02E−03 | 1.53E−03 | – | – | 4.97E−04 | 2.88E−04 | – | – |
| $NO_x$ on $CO_2$ pre-covered samples | 1.06E−03 | 0.86E−04 | 1.33E−04 | 1.68E−04 | 4.83E−04 | 1.19E−04 | 1.24E−04 | – |
| $NO_x/CO_2$ mixtures | 0.90E−03 | 1.21E−03 | 2.87E−04 | 0.742E−04 | 4.63E−04 | 1.04E−04 | 2.02E−04 | – |

On the ternary system, NO can be also originated by $NO_2$ decomposition on Pt sites:

$$NO_2 \rightarrow NO + \tfrac{1}{2}O_2 \qquad (2)$$

As a matter of facts, $O_2$ evolution is observed at the reactor outlet in the case of $Pt\text{-}Ba/Al_2O_3$ catalyst.

It is noted from Fig. 5 that the ratio between $NO_2$ and NO evolved at the reactor outlet is similar in the case of the $NO_2$ admission on the clean and on the pre-carbonated surfaces and slightly lower in the case of the $NO_2/CO_2$ mixture (traces 3). This can be ascribed to the fact that, owing to the competition (although weak) between $CO_2$ and $NO_2$, $NO_2$ can be slightly more efficiently decomposed to NO and $O_2$ by Pt according to reaction (2). This suggestion is supported by the higher $O_2$ evolution in the case of the $NO_2/CO_2$ mixture.

Finally, during the first stages of $NO_2$ storage, when $CO_2$ was present either in the gaseous mixture or pre-adsorbed on the catalyst surface, a $CO_2$ release was also observed (Fig. 5 and Table 2), indicating a displacement of surface carbonates upon $NO_2$ adsorption, as already pointed out by FT-IR data.

A similar behaviour was found for the binary $Ba/Al_2O_3$ sample as well (quantitative data reported in Table 2); however in this case no $NO_2$ decomposition has been observed, as expected.

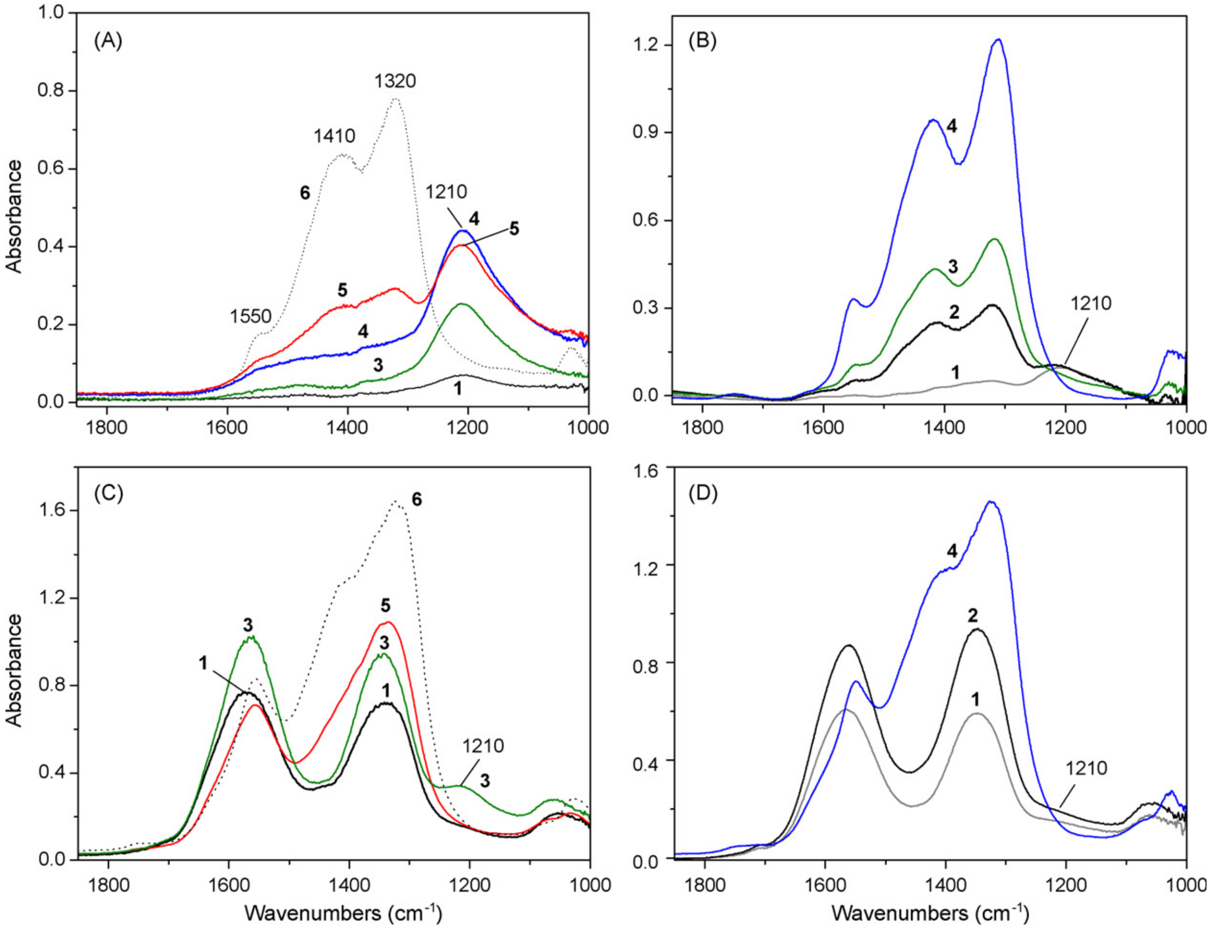

Fig. 6. FT-IR spectra of $Ba/Al_2O_3$ (Sections A and C) and $Pt\text{-}Ba/Al_2O_3$ (Sections B and D) at 350 °C upon admission of 20 mbar of $NO/O_2$ 1:4 mixtures (Sections A and B) or of 36 mbar of $NO/O_2/CO_2$ 1:4:5 mixtures (Sections C and D) at increasing contact time: 10 s (curve 1), 30 s (curve 2), 1 min (curve 3), 5 min (curve 4), 10 min (curve 5), 30 min (curve 6). For sake of clarity some spectra are omitted. Spectra have been reported after subtraction of the spectrum before gas admission.

The results of TPD experiments (data not reported) following the TRM runs with $NO_2/CO_2$ showed an evolution of $CO_2$, along with NO, $O_2$ and $NO_2$, accounting for the presence of small amounts of carbonates not displaced during $NO_2$ storage. The temperature thresholds of $CO_2$ and $NO_x$ desorption agree with the thermal stability of carbonates and nitrates observed by FT-IR.

It is worth of note that no release of $CO_2$ was observed during the TPD runs after TRM experiments with $NO_2$ on clean or pre-carbonated surfaces, indicating that in this case Ba carbonate had been completely displaced by nitrate species during the storage phase, as already suggested by IR data.

All the above findings indicate that at the working temperature $CO_2$ weakly competes with $NO_2$ for the surface oxygen sites, so that $NO_2$ storage can proceed through the ‘‘nitrate route’’ [9], leading to nitrate formation and NO release in the gas phase according to the disproportionation reaction (1), as in the absence of $CO_2$.

As said, very similar results are obtained for Pt-Ba/$Al_2O_3$ and Ba/$Al_2O_3$ catalysts, indicating that Pt is not required to catalyze $NO_2$ storage through ‘‘nitrate route’’. Obviously, Pt is necessary to reoxidize NO released from reaction (1) to $NO_2$.

### 3.2.3. *Adsorption of NO/$O_2$ in the presence of $CO_2$*

IR spectra upon admission of NO/$O_2$ mixtures at 350 °C on Ba/$Al_2O_3$ and Pt-Ba/$Al_2O_3$ catalysts (Fig. 6A and B, respectively) in the absence of $CO_2$ are firstly examined. In both case ionic nitrite species (1210 $cm^{-1}$) were formed at low exposure times and then evolved to nitrates, primarily of the ionic type (1410, 1325 and 1030–1020 $cm^{-1}$) and in minor amounts bridging species (1550 $cm^{-1}$). On the binary system (Fig. 6A) nitrites reached their maximum intensity after 5 min of contact and were still detectable at higher contact time, while nitrates were formed in moderate amounts. Only after 30 min of contact (Fig. 6A, curve 6) nitrites were no more detected and nitrates were present in significant amounts. Conversely, on the ternary system (Fig. 6B) nitrites reached their maximum intensity already after 30 s of contact and were completely disappeared thereafter, so that after few minutes of contact only nitrates were present on the catalyst surface, similar in nature and amounts to those obtained upon $NO_2$ admission.

When $CO_2$ was added to the NO/$O_2$ mixture (Fig. 6C and D for the binary and ternary samples, respectively) bidentate carbonates were immediately formed along with nitrite species (curves 1). On increasing the contact time, carbonates were partially displaced, as indicated by the intensity decrease of the bands at 1560 and 1060 $cm^{-1}$, while nitrites evolved to nitrate species (curve 2–6).

Notably, on the binary system (Fig. 6C) large amounts of carbonates were still present at the surface after several minutes of exposure to the NO/$O_2$/$CO_2$ mixture (see, *e.g.* curve 5 of Fig. 6C). Conversely, on the ternary system (Fig. 6D) a large fraction of carbonates initially formed was displaced upon $NO_x$ storage, so that after few minutes of exposure to the NO/$O_2$/$CO_2$ mixture the amount of nitrates stored was comparable to that obtained in the absence of $CO_2$.

A significant finding is that, both on the binary and on the ternary systems, the amount of surface nitrites present at each contact time is lower in the presence than in the absence of $CO_2$ (compare Fig. 6C with A and Fig. 6D with B). This indicates that $CO_2$ competes for the surface oxygen sites able to give nitrites.

Also in this case it is possible to obtain a rough evaluation of the relative amounts of carbonates and nitrates by examining the stability of surface species upon evacuation at 450 °C. As seen from Fig. 3, both on the binary and on the ternary systems the stability of species formed upon admission of the NO/$O_2$/$CO_2$ mixture is roughly intermediate between those of species formed upon admission of NO/$O_2$ on one hand and of $CO_2$ on the other hand.

In another series of experiments, NO/$O_2$ was admitted on the catalyst surface previously saturated by $CO_2$ at 350 °C and thereafter evacuated at the same temperature (Fig. 7). Both on Ba/$Al_2O_3$ and Pt-Ba/$Al_2O_3$ samples carbonates initially present were progressively displaced on increasing the exposure time to the NO/$O_2$ mixture. In parallel, nitrites were formed at low contact time and then evolve to nitrates. As in the case of NO/$O_2$ adsorption on the clean surfaces, nitrites were still

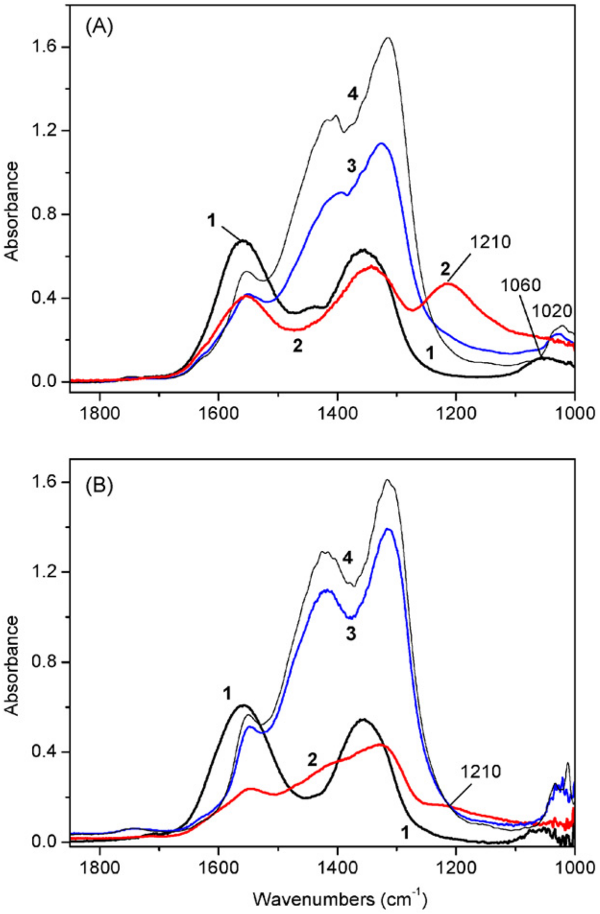

Fig. 7. FT-IR spectra of Ba/$Al_2O_3$ (Section A) and Pt-Ba/$Al_2O_3$ (Section B) after admission of 20 mbar of $CO_2$ at 350 °C and subsequent evacuation at 350 °C (curve 1); subsequent admission of 20 mbar of NO/$O_2$ 1:4 mixtures at 350 °C after 1, 5 and 10 min of contact (curves 2, 3 and 4, respectively). Spectra have been reported after subtraction of the spectrum before gas admission.

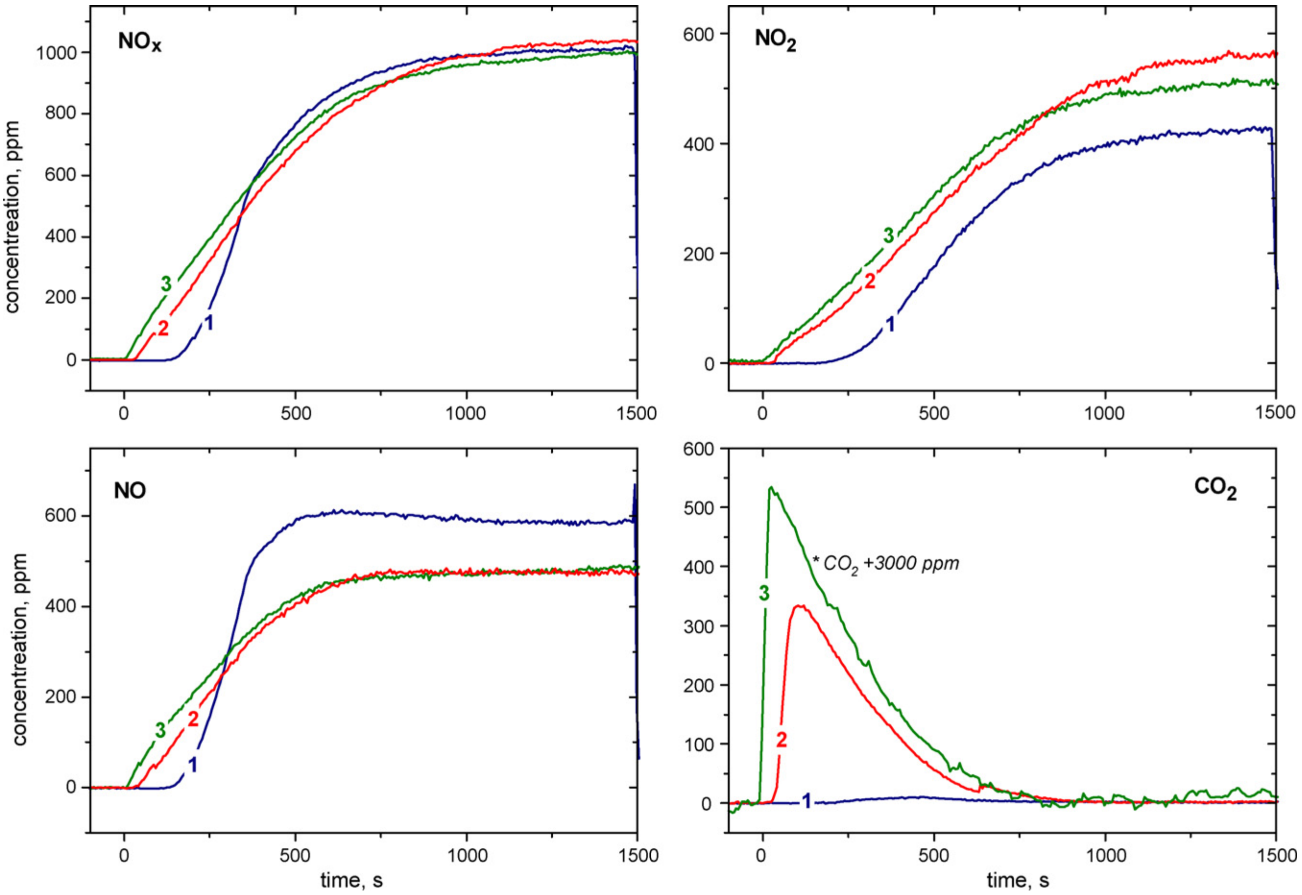

Fig. 8. $NO_x$, $NO_2$, NO, $CO_2$ outlet concentration *vs.* time on Pt-Ba/γ-$Al_2O_3$ catalyst determined by TRM experiments at 350 °C upon admission of NO/$O_2$ (curve 1), NO/$O_2$ on $CO_2$ pre-covered sample (curve 2) and NO/$O_2$/$CO_2$ mixture (curve 3).

detectable on the Ba/$Al_2O_3$ sample after several minutes of contact (Fig. 7A), while on the ternary system only nitrates are present after 30–60 s of contact (Fig. 7B).

TRM results obtained over Pt-Ba/$Al_2O_3$ sample upon NO/$O_2$ admission at 350 °C (Fig. 8) indicated that $NO_x$ species were stored with a significant breakthrough (*i.e.* a period of complete $NO_x$ uptake). After breakthrough (200 s), both NO and $NO_2$ were observed at the reactor outlet.

In the presence of $CO_2$ (traces 2 and 3 of Fig. 8) the $NO_x$ breakthrough is significantly shortened and the $NO_x$ adsorption process is slower. However, in spite of the significant reduction of the $NO_x$ breakthrough, quantitative data obtained at saturation showed that the $NO_x$ storage capacity upon admission of NO/$O_2$/$CO_2$ mixtures or upon admission of NO/$O_2$ over the $CO_2$ pre-covered catalysts was only slightly lower than that observed in the absence of $CO_2$ (Table 2). In all cases, the $NO_x$ storage capacity of the ternary catalyst was markedly higher than that of the binary system.

In line with IR results, $NO_x$ adsorption was accompanied by evolution of $CO_2$. A release of $CO_2$ was also observed during TPD that follow TRM experiments. This fact confirms that carbonate species had been only partially displaced during the NO/$O_2$ storage phase. All the above data concerning NO storage in the presence of oxygen on Pt-Ba/$Al_2O_3$ catalyst can be summarized and interpreted as follows: (i) NO is activated over reactive surface oxygen ions of the Ba oxide phase (*e.g.* $O^{2-}$, $O_2^{-}$), while $O_2$ is dissociated by Pt sites and atomic oxygen transferred to the neighboring Ba sites; (ii) NO is thus stored primarily in the form of nitrites, which are then progressively oxidized to nitrates (“nitrite route”) [9]. The close proximity between Pt and Ba, previously evidenced [9,12], will favor NO/$O_2$ storage through the “nitrite route”. Pt is observed to promote both the formation of nitrites and their oxidation to nitrates. Moreover, Pt also promotes NO oxidation to $NO_2$, thus the above “nitrite” pathway operates simultaneously with the $NO_2$ storage through “nitrate route”, already proposed for $NO_2$ adsorption.

When gaseous $CO_2$ is added to NO/$O_2$ mixture, $CO_2$ is immediately adsorbed to form carbonates, thus competing with NO for the surface Ba oxygen ions. Carbonates are then only partially displaced, so that the amount of nitrites formed is lower than in the absence of $CO_2$. It appears therefore that “nitrite route” is in some extent inhibited by the presence of $CO_2$. Notably, the $NO_x$ breakthrough is significantly shortened in the presence of $CO_2$, so that the extent of $NO_x$ breakthrough can be tentatively associated with the occurrence of the “nitrite route”. However, in the case of Pt-Ba/$Al_2O_3$ catalyst, NO can be oxidized to $NO_2$ by Pt and $NO_2$ can be stored in the form of nitrates through the “nitrate route'', which is not significantly affected by the presence of $CO_2$, as previously shown.

## 4. Conclusions

The combined use of *in situ* FT-IR spectroscopy and the transient response method has provided complementary information which allowed the proposal of a pathway for $NO_2$ and $NO/O_2$ storage in the absence and in the presence of $CO_2$.

The picture obtained upon admission of $NO_2/CO_2$ mixtures or of $NO_2$ on the catalyst surface previously saturated with $CO_2$ strictly parallels the results collected in the case of $NO_2$ adsorption in the absence of $CO_2$. The collected results indicate that, also in the presence of high amounts of $CO_2$, Pt-Ba/$Al_2O_3$ catalysts are able to efficiently perform $NO_x$ storage through a pathway that involves the formation of surface nitrate species (''nitrate route'').

In the case of the storage of NO and $O_2$, two pathways operating simultaneously are proposed: the ''nitrite route'', that involves the initial formation of surface nitrite and their subsequent evolution to nitrates, and the ''nitrate route'', that involves NO oxidation to $NO_2$ over Pt and its subsequent adsorption on Ba phase in the form of nitrates. In the presence of $CO_2$, if ''nitrite route'' is in some extent inhibited due to the competition between NO and $CO_2$ for the surface oxygen sites of the Ba phase, ''nitrate route'' can proceed as in the absence of $CO_2$. It turns out that also in this case Pt-Ba/$Al_2O_3$ catalysts are able to efficiently perform $NO_x$ storage.

## References

[1] N. Miyoshi, S. Matsumoto, K. Katoh, T. Tanaka, J. Harada, N. Takahashi, K. Yokota, M. Sugiura, K. Kasahara, SAE Technical Paper 950809, 1995.

[2] S. Matsumoto, Catal. Today 29 (1996) 43.

[3] N. Takahashi, H. Shinjoh, T. Iijima, T. Suzuki, K. Yamazaki, K. Yokota, H. Suzuki, N. Miyoshi, S. Matsumoto, T. Tanizawa, T. Tanaka, S. Tateishi, K. Kasahara, Catal. Today 27 (1996) 63.

[4] H. Shinjoh, N. Takahashi, K. Yokota, M. Sugiura, Appl. Catal. B 15 (1998) 189.

[5] N.V. Cant, M.J. Patterson, Catal. Today 73 (2002) 271.

[6] C. Hess, J.H. Lunsford, J. Phys. Chem. B 106 (2002) 6358.

[7] H.Y. Huang, R.Q. Long, R.T. Yang, Energy Fuels 15 (2001) 205.

[8] P. Broqvist, I. Panas, E. Fridell, H. Persson, J. Phys. Chem. B 106 (2002) 137.

[9] I. Nova, L. Castoldi, F. Prinetto, G. Ghiotti, L. Lietti, E. Tronconi, P. Forzatti, J. Catal., 222/2 (2004) 377.

[10] I. Nova, L. Castoldi, F. Prinetto, V. Dal Santo, L. Lietti, E. Tronconi, P. Forzatti, G. Ghiotti, R. Psaro, S. Recchia, Topics Catal., 30/31 (2004) 181.

[11] F. Prinetto, G. Ghiotti, I. Nova, L. Castoldi, L. Lietti, P. Forzatti, Phys. Chem. Chem. Phys. 5 (20) (2003) 4428.

[12] F. Prinetto, G. Ghiotti, I. Nova, L. Lietti, E. Tronconi, P. Forzatti, J. Phys. Chem. B 105 (2001) 12732.

[13] L. Castoldi, I. Nova, L. Lietti, P. Forzatti, Catal. Today 96 (2004) 43.

[14] K. Nakamoto, Infrared and Raman Spectra of Inorganic and Coordination Compounds, fourth ed., Wiley, New York, 1986.

[15] P. Pascal, Nouveau Traité de Chimie Minér ale, Masson, Paris, 1958.

[16] J.C. Lavalley, Catal. Today 27 (1996) 377.

[17] C. Morterra, G. Magnacca, Catal. Today 27 (1996) 497.

[18] T. Szailer, J.H. Kwak, D.H. Kim, J. Szanyi, C. Wang, C.H.F. Peden, Catal. Today 114 (2006) 86.

[19] D.H. Kim, Y.H. Chin, J.H. Kwak, J. Szanyi, C.H.F. Peden, Catal. Lett. 105 (2005) 259.

[20] J. Szanyi, J.H. Kwak, J. Hanson, C. Wang, T. Szailer, C.H.F. Peden, J. Phys. Chem. B 109 (2005) 7339.

[21] L. Lietti, P. Forzatti, I. Nova, E. Tronconi, J. Catal. 204 (2001) 175.